Ibn Al-Haitham Journal for Pure and Applied Sciences
Journal homepage: jih.uobaghdad.edu.iq
PISSN: 1609-4042, EISSN: 2521-3407
IHJPAS. 2026; 39(1)

Improvement of Structural and Optical Properties of ZnO1-xAgOx Nano Composite Thin Film Using Pulsed Laser Deposition

Safaa E. Husain[1*] and Lamia K. Abbas[2]
[1,2] Department of Physics, College of Science, University of Baghdad, Baghdad, Iraq
*Corresponding Author

Received:22/May/2025.
Accepted: 28/August/2025.
Published:20/January/2026.
doi.org/10.30526/39.1.4206

Abstract

Thin films of ZnO1-xAgOx nanostructures were successfully deposited on glass substrates using pulsed laser deposition with varying AgO nanoparticle concentrations. Structural and optical characterizations were performed to evaluate the effect of AgO incorporation. XRD patterns confirmed a hexagonal polycrystalline structure, with additional peaks for cubic silver or silver oxide due to AgO inclusion. Crystal size slightly increased at x = 0.05 and 0.25, indicating enhanced growth, while it decreased at other ratios due to lattice strain and defects. FTIR analysis showed Zn–O stretching modes, hydroxyl, carbon-based groups, and Ag–O bands, confirming successful incorporation. AFM results revealed reduced surface roughness with low AgO ratios, followed by increased roughness at x = 0.25 and 0.30. Optical transmittance decreased, while absorption increased with AgO, and the optical band gap narrowed from 3.2 eV to 2.2 eV. Hall Effect measurements indicated reduced n-type carrier concentration, suggesting a shift toward p-type conductivity via acceptor level formation.

Keywords: Semiconductors, Pulse Laser Deposition, AgO, ZnO Nanoparticle, ZnO1-xAgOx Nanocrystallain, Thin Films.

1. Introduction

Nanotechnology is one of the most advanced and perspective types of the modern technology which serves a wide range of applications in medicine, electronics and environmental science. It deals with the manipulation of materials at the nanoscale where particles have distinct physical and chemical properties as a result of the high surface area per volume and quantum effect [1]. These attributes have made it possible to improved considerable alterations in the different industrial and biomedical areas[2]. Zinc oxide (ZnO), which is a well-known n-type semiconductor, has gained much attention thanks to a wide band gap, a high exciton binding energy, and outstanding chemical and thermal stability. Specifically, ZnO nanoparticles show superior performance over the bulk form and they have multiple glorious applications in optoelectronics, energy storage, photocatalysis, and gas sensing[3,4].

ZnO is commonly doped or mixed with other materials in order to differentiate the properties that this material exhibit. Such a material is silver oxide (AgO) which is known for its unique optical electrical properties, and antimicrobial properties. AgO is one of the phases of silver oxides (including Ag_2O, Ag_2O_3, Ag_3O_4, Ag_4O_3, Ag_4O_4) and is the most thermodynamically stable phase. It has a simple cubic crystal structure at room temperature and acts as a transparent p-type semiconductor with a band light ranging from 1.5 to 3.2 eV [5,6] at room temperature. AgO has attracted the attention of researchers due to its prospects of being used as gas sensors, antimicrobial coatings, photovoltaics, and photodiodes.

The fabrication of thin films is an integral part of the nanomaterial development. Once of the techniques in preparing thin films involves chemical vapor deposition (CVD), magnetron

sputtering, spray pyrolysis, molecular beam epitaxy (MBE), sol-gel processing, and pulsed laser deposition (PLD)[7] .PLD, one of them, provides some unique benefits including: precise stoichiometric control, high deposition rate, as well as capability to deposit good quality films even in relatively low substrate temperature[8]. In this study ZnO thin films of various ratios with AgO were synthesized using the method of PLD technique. The objective is to consider the structural and optical properties of the end films and to understand the effect of the content of AgO with major focus on possible applications in sensors and optoelectronic micro-lamps, as well as in photo detectors, solar cells, transparent conductive films, and photocatalytic devices.

2. Materials and Methods

In this study, five types of compositions were prepared with an AgO content of: x (0, 0.05, 0.15, 0.25 and 0.30). The source materials – high-purity zinc oxide (ZnO) and silver oxide (AgO) (purity: 99.9%) were supplied by Aldrich. Each of the compositions was precisely weighed according to its Weight ratio on a four-digit electronic balance (10^{-4} g precision). Received mixtures were pre-weighed and loaded into quartz ampoules with a height of about 30 cm and inner diameter of 8 mm. The ampoules were subjected to vacuum level of ~10^{-3} Torr and then closed before being heated in a furnace at 900 °C for 5 hours to obtain solid-state reaction (sintering). Following the heat treatment, the samples were cooled down to the room temperature.

The sintered materials, after that, were ground into powders to achieve the uniformity, and then were pressed in pellets of 1 cm in diameter and 0.5 cm in thickness. There was the use of a hydraulic press which subjected the sample to a pressure of 7 tons for duration of 15 minutes.

The thin film deposition was conducted at the vacuum of 2 x 10^{-2} of Torr by the use of the pulsed Nd: YAG laser. The laser had the energy of 540 mJ per pulse, a repetition rate of 6 Hz and a total, respectively, of 250 pulses. The laser beam was focused in a quartz window with an incident angle of 45° at the surface of the target pellet. Deposition of the ablated material was carried out on pre-cleaned glass substrates of dimensions 1.2 × 2.5 × 75 mm.

3. Results

3.1. Structural Characterization

Using XRD, the structural properties of $ZnO_{1-x}AgO_x$ (x = 0.0 to 0.30) thin films were examined, as can be seen in **Figure 1**. The 2θ range varies from 20° to 80°. The diffraction spectra were recorded. For the undoped ZnO sample, the dominant peaks were observed at 2θ ≈ 31.8°, 34.4°, and 36.2° for (100), (002), and (101) planes, respectively, indicating typical hexagonal wurtzite and a polycrystalline nature of the films, This is consistent with the results obtained on nanostructured ZnO/SnO_2 films[9].After doping with AgO nanoparticles, the additional peaks appeared, especially at 2θ ≈38.1° and 44.2° referring to cubic silver (Ag), (111) and (200) planes respectively. The raising intensity of these peaks with increased AgO content again upholds the successful incorporation of AgO and the creation of a different crystalline phase on ZnO matrix. This implies that structural ordering is promoted by the presence of AgO doping and also leads to better crystallinity at particular doping concentrations. If we compare one of the peaks, such as the peak belonging to plane (200), we notice that the increase in doping led to: The FWHM increases, which means that the doping led to an increase in the width of the peaks, indicating that the crystalline structure has transformed into a nanostructure, and this is what we will notice in the remaining tests. From the **Table 1** we also notice that the interplanar distance d_{hkl} decreases with doping. This means that doping leads to shifting the peaks towards high 2θ according to Bragg's diffraction law. This matches the table, as we observe that the undoped films had the peak position belonging to the (200) plane at 2θ = 34.42, and after doping at x = 0.25, the position of this peak shifted to 2θ = 44.23.

The average crystallite size (D) was determined based on Scherrer's **Equation 1** [10]:

$$D = 0.9\lambda / (\beta \cos\theta) \quad \textbf{(1)}$$

where λ is the X-ray wavelength (in Å), β is the full width at the half maximum (FWHM) of the diffraction peak (in rad.) and θ, the Bragg diffraction angle. By calculating the value of D from Scherrer's equation, increasing the doping with silver oxide leads to a decrease in the average crystallite size, probably due to greater lattice strain or the existence of defects in the structure, preventing the development of crystals. This confirms that the doping is more indicative of the transformation of the crystalline structure into a nanostructure. Dislocation density (δ) as an expression for the number of crystal imperfections was also calculated according to the following relation[11].

$$\delta = 1 / D^2 \quad \textbf{(2)}$$

It was shown that doping led to an increase in the δ values, which means an increase in crystalline defects, as doping may lead to the formation of voids or dangling bonds, or it may lead to a distortion in the lattice crystal structure due to the difference in the ionic radius of the zinc and silver ions.

Table 1. The parameters of the XRD pattern of $ZnO_{1-x}AgO_x$ nanocrystall thin films at different ratios of AgO (0, 0.05, 0.15, 0.25 and 0.3)

Ag%	2θ (Deg.)	FWHM (Deg.)	d_{hkl} (Å)	D (nm)	$\delta=1/D^2(nm^{-2})$	(hkl)	Phase	Card No.
0	31.79	0.2539	2.8124	32.54	0.0009	(100)	Hex.ZnO	96-901-1663
	34.42	0.2077	2.6032	40.060	0.0006	(002)	Hex.ZnO	96-901-1663
	36.29	0.2539	2.4730	32.941	0.0009	(101)	Hex.ZnO	96-901-1663
	47.57	0.2539	1.9097	34.208	0.0008	(102)	Hex.ZnO	96-901-1663
	56.64	0.3	1.6235	30.093	0.0011	(110)	Hex.ZnO	96-901-1663
	62.87	0.277	1.4768	33.625	0.0008	(103)	Hex.ZnO	96-901-1663
	67.97	0.323	1.3779	29.672	0.0011	(112)	Hex.ZnO	96-901-1663
	69.13	0.3692	1.3577	26.137	0.0014	(201)	Hex.ZnO	96-901-1663
0.05	31.78	0.2308	2.8127	35.805	0.0007	(100)	Hex.ZnO	96-901-1663
	34.44	0.2308	2.6015	36.053	0.0007	(002)	Hex.ZnO	96-901-1663
	36.29	0.2308	2.4733	36.238	0.0007	(101)	Hex.ZnO	96-901-1663
	38.18	0.3693	2.3550	22.774	0.0019	(111)	Cub. Ag	96-901-2432
	67.97	0.3692	1.3779	25.959	0.0014	(112)	Hex.ZnO	96-901-1663
	69.10	0.3	1.3581	32.162	0.0009	(201)	Hex.ZnO	96-901-1663
0.15	31.746	0.2539	2.8163	32.544	0.0009	(100)	Hex.ZnO	96-901-1663
	34.44	0.2308	2.6015	36.05	0.0007	(002)	Hex.ZnO	96-901-1663
	36.24	0.2308	2.4763	36.23	0.0007	(101)	Hex.ZnO	96-901-1663
	38.16	0.2538	2.3563	33.135	0.0009	(111)	Cub. Ag	96-901-2432
	44.32	0.323	2.0420	26.568	0.0014	(200)	Cub. Ag	96-901-2432
	68	0.3461	1.3775	27.69	0.0013	(112)	Hex.ZnO	96-901-1663
	69.17	0.3692	1.3569	26.145	0.0014	(201)	Hex.ZnO	96-901-1663
0.25	31.74	0.2077	2.8164	39.78	0.0006	(100)	Hex.ZnO	96-901-1663
	32.32	0.3231	2.7674	25.61	0.0015	(111)	Cub.Ag2O	96-101-0605
	36.23	0.1846	2.4770	45.300	0.0004	(101)	Hex. ZnO	96-901-1663
	38.16	0.2538	2.3563	33.135	0.0009	(111)	Cub. Ag	96-901-2432
	44.23	0.2769	2.0460	30.981	0.0010	(200)	Cub. Ag	96-901-2432
	64.46	0.5539	1.4441	16.961	0.0034	(220)	Cub. Ag	96-901-2432
	34.44	0.2769	2.6015	30.05	0.0011	(002)	Hex. ZnO	96-901-1663
0.3	36.22	0.2308	2.4777	36.231	0.0007	(101)	Hex. ZnO	96-901-1663
	38.13	0.2076	2.3577	40.507	0.0006	(111)	Cub. Ag	96-901-2432
	44.39	0.2307	2.0390	37.207	0.0007	(200)	Cub. Ag	96-901-2432
	47.55	0.2307	1.9105	37.645	0.0007	(102)	Hex. ZnO	96-901-1663
	69.08	0.3461	1.3585	27.874	0.0012	(201)	Hex. ZnO	96-901-1663
	77.48	0.3231	1.2308	31.531	0.0010	(311)	Cub. Ag	96-901-2432

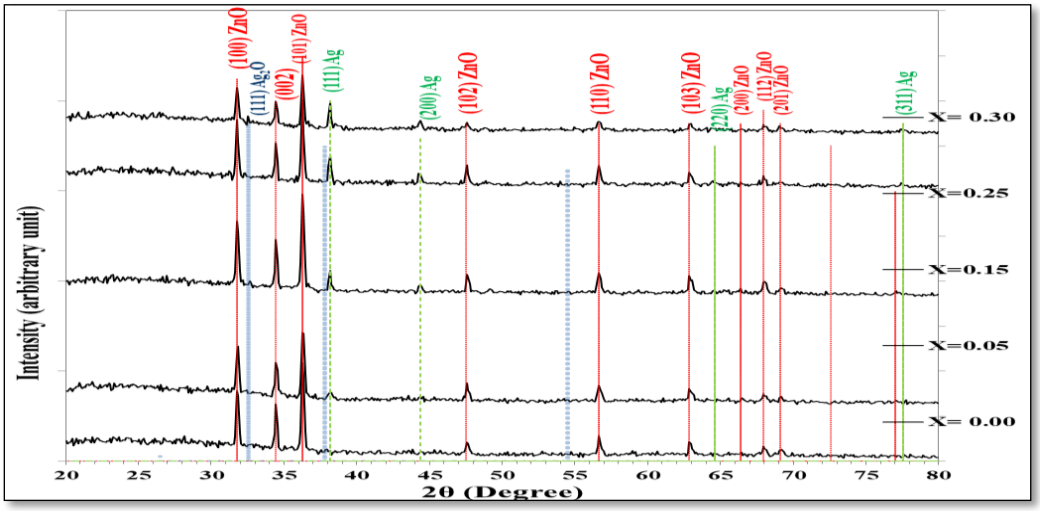

Figure 1. XRD patterns of the ZnO $_{1-x}$AgO$_x$ nanocrystall thin films at different ratios of AgO (0, 0.05, 0.15, 0.25 and 0.3).

3.2. FTIR Analysis

Analyzes of FTIR were done to determine the way in which the chemical structure is played from the presence of AgO in ZnO. The results indicated that the vibrational modes of ZnO were greatly changed in the presence of AgO, and this has a strong indication of a strong interaction between the two materials. It can improve the properties of the material for use in catalysis, for example, and sensor technology.

FTIR spectrum of the prepared samples displays dominant absorption peaks indicating chemical reactions that take place on the surface of the material. **Figure 2** gives the FTIR spectra of ZnO $_{1-x}$ AgO$_x$ Nano crystalline thin films with different AgO ratios (x = 0.05, 0.15, 0.25, and 0.30) under ambient temperature versus wavenumber in the 500–3500 cm^{-1} range.

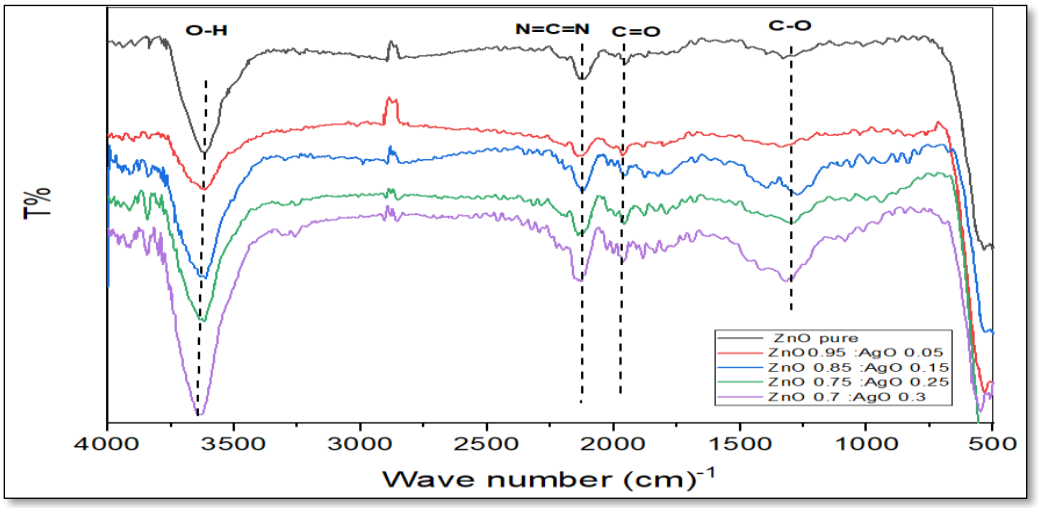

Figure 2. FTIR spectra of the ZnO $_{1-x}$ AgO$_x$ Nano crystall thin films at different ratios of AgO (0, 0.05, 0.15, 0.25 and 0.3) at room temperature.

In **Figure 2**, it can be seen that polymorph ZnO $_{1-x}$ AgO$_x$ has four unique bands. The spectrum displays a wide surface containing maximum intensity in the 3500–3000 cm^{-1} which is ascribed to the stretching vibrations of the ZnO hydroxyl group (- OH) attached onto the ZnO surface. This peak is an indicator of the adsorption of water on the surface or the formation of hydroxyl groups in the course of the preparation method [12]. With the increase in the quantity of AgO, we observed a slight downshift in the intensity of this peak indicating that AgO is interacting with the surface groups of ZnO and diminishing the capacity of moisture to be adhered to the surface.

Another novelty peaks are represented by the absorption peaks at 2854 cm-1 and 2924 cm-1 for the samples, which signals chemical residuals from solvents or organic ligands adhered on the ZnO surface. This is what was observed, when preparing ZnO–AgO with oleic acid as a coating agent, these peaks are observed [13]. The 1581cm⁻¹ peak, possibly from organic residues or this being an interaction between ZnO and AgO [14], signifies the vibrations of the carboxyl group (COO-). It is reported that, this peak transferred from 1707 cm⁻¹ for pure oleic acid to 1545–1581 cm⁻¹ for doped with ZnO indicating that a COO–Zn bond is formed . The fact that chemical impurities and residues of organic compounds used in the preparation are likely the cause of appearance of the absorption band at ~2200 cm⁻¹; (N=C=N stretching [15]. There was no significant change in this peak after introduction of AgO which means that the doping process could not have much effect on these functional groups. The absorption peak at 500–600 cm⁻¹ indicates stretching vibrations of the Zn–O link, which indicates that the ZnO structure was also maintained after the incorporation of AgO [16]. There were no significant shifts in peak position, where silver doping did not change the basic structure of ZnO. New peaks are seen at the 600-700 cm⁻¹ range which is that due to Ag-0 vibrations. These peaks show the interaction of AgO with ZnO but not creating a strong bond that changes the ZnO structure to a greater extent.

3.3. The Atomic Force Microscopy (AFM) Images

AFM images of the undoped ZnO film, and ZnO doped with different concentrations of AgO (0.05, 0.15, 0.25, 0.3) have been shown below in the figure. AFM analysis gives a two dimensional i.e., topographic 2D images of the surface of the specimen which gives a good insight of surface properties like roughness. **Figure 3.a** presents an AFM image of an undoped ZnO film, for pure Zinc Oxide the surface roughness values were 13.67 nm, with the RMS roughness values being 17.42 nm, also the difference between the highest peak and valleys was 170.1 nm (**Table 2**). These results are consistent with the results obtained by [17]. When the introduction of AgO at a concentration of 0.05 was performed as demonstrated in **Figure 3.b**, the surface was highly smoothed and the roughness of the surface was reduced to 7.3 nanometer with RMS of 13 nanometer while the gap between the highest peak and lowest valley was reduced to 171 nanometers signifying that the surface had become more evenly & smoother.

With the increase in AgO ratio up to 0.15 as displayed in **Figure 3.c**, there was no significant change in the roughness of the deposited films, which resulted in reduction to even 6.8 nanometers, and RMS roughness was also decreased to 12.5 nanometers. However, small decrease in difference between the peak and the valley was observed, as it came down to the 160 nanometer, this is what was also noted by researcher [18]. This over all roughness with addition of small amounts of AgO implies a better surface uniformity and also consistency. Upon increasing the doping up to 0.25 see **Figure 3.d,** there was also an increase of roughness, up to 12.4 nanometers with an RMS of 23.9 nanometers and an apparent increase in the difference between the highest peak and the deepest valley had an increase of 218 nanometers). Upon increasing the doping to further 0.3 as illustrated in **Figure 3.e** with AgO, there was an increased roughness, varying to 29.6 nanometers and RMS to 51.2 nanometers and augmented rise in the difference between the peak top and the minimum dip being 717 nanometers. These results are consistent with the results previous study [19].

Table 2. Average of the surface roughness and the granular size for the prepared films (ZnO: AgO) by means of the AFM surface topography

Sample	Roughness (nm)	RMS (nm)	Peak peak (nm)
ZnO pure	13.67	17.4	170.1
($ZnO_{0.95} - AgO_{0.05}$)	7.3	13	174
($ZnO_{0.85} - AgO_{0.15}$)	6.8	12.5	160
($ZnO_{0.75} - AgO_{0.25}$)	12.4	23.9	218
($ZnO_{0.7} - AgO_{0.3}$)	29.6	51.2	717

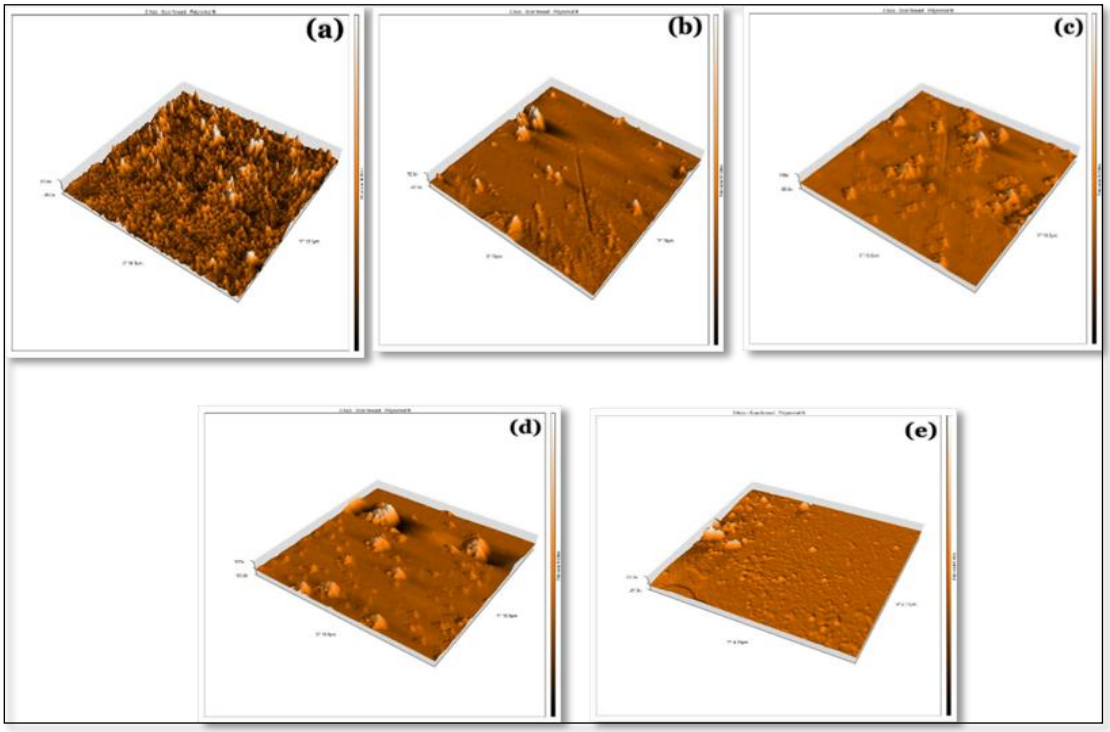

Figure3. The 2D AFM images of the (a) undoped ZnO and ZnO films doped with (b) 0.05% AgO, (c) 0.15% AgO, (d) 0.25% AgO and (e) 0.3% AgO

3.4. Optical Properties

UV-Vis spectroscopy was used for determining the optical properties of ZnO $_{1-x}$ AgO_x (non-stoichiometric) thin films deposited onto glass substrates at high temperatures employing the pulsed laser deposition (PLD) technique. **Figures 4** and **5** show the optical transmission and absorption spectra if the films in the range of 300-1100 nm. The pure ZnO film had a transmittance of about 34.83% in the visible region of 500 nm. The increase of AgO in the water caused progressive decrease in the transmittance reaching to 13.86% at x=0.30. This drop in transmittance is probably the result of the enhanced absorption and light scattering produced by Ag0 nanoparticles, and that may modify the surface morphology and increase the number of localized states [20]. In addition, AgO incorporation tends to decrease the surface roughness, increase the surface uniformity and alters the light transmission properties of the cellulose. At the absorption behavior, a clear dependency of the absorption coefficient (α) on the increase of AgO ratio was observed that the absorption coefficient value was equal to 11720 cm^{-1} for the undoped film, i.e. when x = 0.00. Then this value increased to 21955 cm^{-1} by increasing the silver oxide doping ratio to x = 0.30. This increase in absorption might be linked to the nanostructured phase of AgO which enhances the effective surface area and thus increases the interaction of the phase with the incident light.Moreover, pure ZnO has high UV absorption since it has a large direct band gap, while doping with AgO does not introduce defect states that can absorb light at a larger range [21].

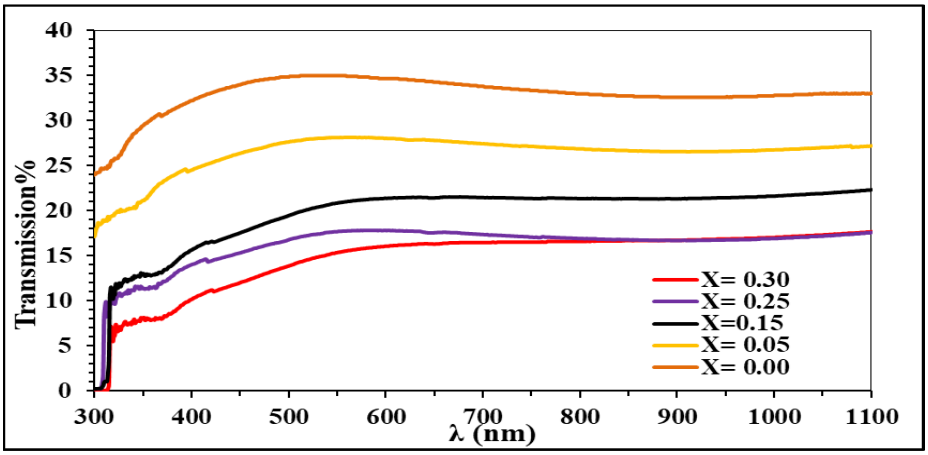

Figure 4. Shows the transmittance spectrum as a function of wavelength for $(ZnO)_{1-x}$ $(AgO)_x$ thin films produced using the PLD process

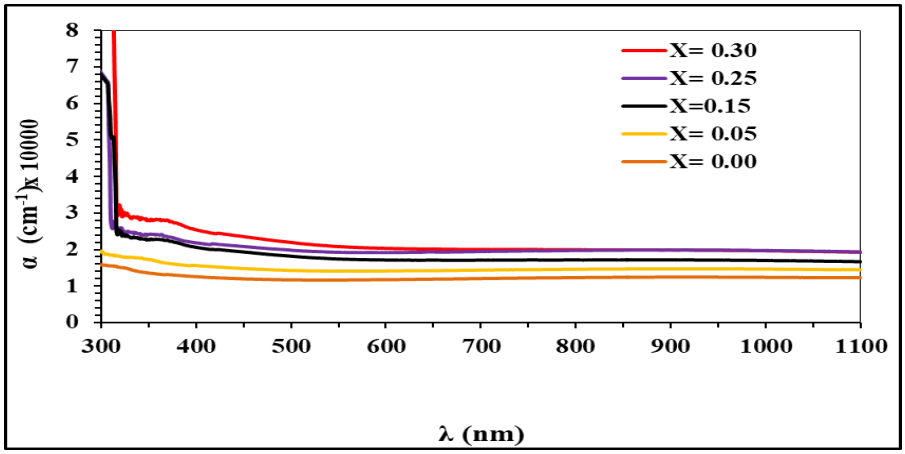

Figure 5. Shows the absorption spectra for ZnO_{1-x} : AgO_x thin films produced using the PLD process at various doping ratios.

The optical band gap of thin films was determined using Tauc's formulation. To calculate Tauc plots for ZnO_{1-x}: AgO_x thin films, one should make Tauc plots, which involve plotting $(\alpha\ h\ \nu)^2$ vs incoming photon energy $(h\ \nu)$. The equation used to determine the optical energy band gap *Eg* using Tauc's equation is graphs are used:

$$(\alpha\ h\ \nu) = B\left(h\nu - E_g\right)^{1/r} \quad (3)$$

Absorption coefficient (α) is given as α=2.303 *(A/d)* where *A* is optical absorbance and *d* is the thickness of the thin film, *B* is constant, *hν* is the photon energy, *Eg* (is the optical energy gap) and *r* is the transition type which =1/2 for allowed direct transition. **Figure 6** shows the graph of $(\alpha\ h\ \nu)^2$ vs. *hν* for $(ZnO)_{1-x}$: $(AgO)_x$ thin films at varying dopant ratio of the AgO NPs (0, 0.1, 0.2) %.

Table 3.The transmittance, absorption coefficient at λ=550nm, and optical energy gap of $(ZnO)_{1-x}$ $(AgO)_x$ thin films prepared by PLD technique.

AgO % x	T%	α (cm^{-1})	Eg (eV)
0.00	34.83	11720	3.20
0.05	27.63	14291	2.80
0.15	19.45	18194	2.30
0.25	16.76	19845	2.20
0.30	13.86	21955	2.20

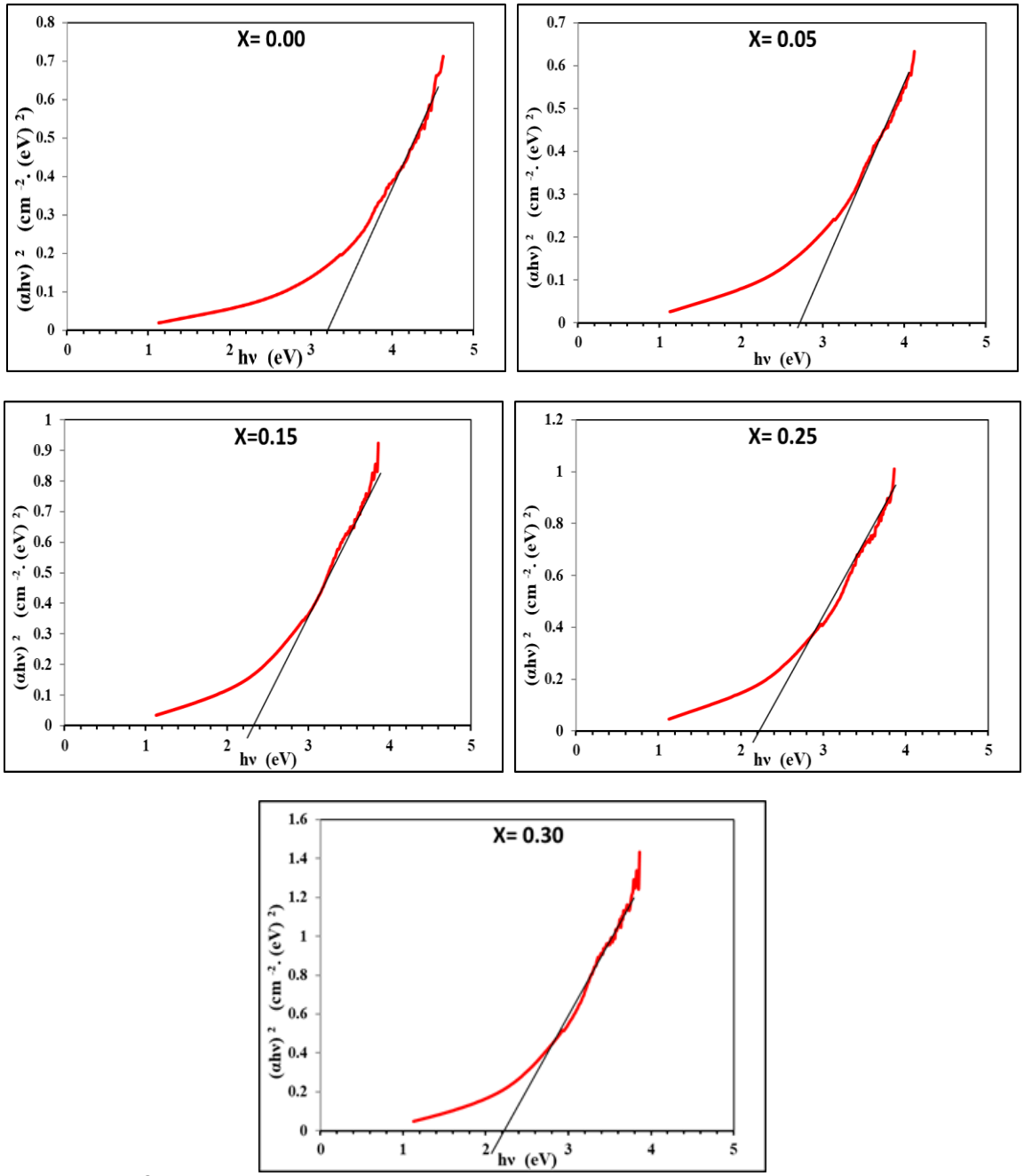

Figure 6. $(\alpha\, h\, \upsilon)^2$ against $(h\, \upsilon)$ for $(ZnO)_{1-x}$ $(AgO)_x$ thin films with varying doping ratios generated using PLD technology.

The Tauc plot method was used to obtain the optical energy band gap (*Eg*) values, as indicated in **Table 3.** The results of the optical measurements are consistent with the results obtained by the previous study [22]. The band gap decreased from 3.20 eV for the film undoped ZnO to 2.20 eV for x = 0.30. This redshift is said to arise due to the scattering of the electronic states of ZnO and AgO that results in defect levels and microstrains in the crystal lattice[23-25] . These structural defects create localized states in the band gap that cause band narrowing and a reduction in the optical energy gap, thus in good agreement with earlier literature reports [26-28].

3.5. Hall Effect Measurements

Hall effect measurements were performed on $(ZnO)_{1-x}(AgO)_x$ thin films prepared by the PLD method to determine the type, concentration and mobility of charge carriers and to study the extent to which these values are affected by AgO doping as shown in **Table 4.**

Table 4. The results of the Hall Effect calculations for ZnO_{1-x} : AgO_x thin films produced using the PLD process at various doping ratios

AgO % X	μ_H ($cm^2/V{\cdot}s$)	n_H (cm^{-3})	Type
0	212.9	1.88	n
0.05	70.95	9.11	p
0.15	21.29	188.0	p
0.25	117.6	10.49	p
0.3	180.5	3.24	p

The measurements revealed that the undoped ZnO film exhibited n-type conductivity with a low carrier concentration (1.88×10^{12} cm^{-3}) and high relative mobility (212.9 $cm^2/V{\cdot}s$), indicating a high degree of crystallinity and low levels of acceptor-like defects. When AgO was added, the films showed a transition from n-type conductivity to p-type in most samples. This transition indicates the formation of donor levels due to the incorporation of Ag^+ into the ZnO lattice, which acts as p-type additives. The p-type samples showed significant variation in carrier concentration and mobility. For example, the film with x = 0.15 showed the highest carrier concentration (188×10^{12} cm^{-3}), while the film with x = 0.25 showed a much lower carrier concentration (10.49×10^{12} cm^{-3}), indicating that an excess of AgO beyond the optimal ratio may lead to an increase in scattering centers or structural disorder that hinders carrier movement. These results are consistent with the structural (XRD) and optical (UV-Vis) analyses. The transition to p-type conductivity corresponds to the appearance of secondary phases associated with silver in X-ray diffraction (XRD) analysis and the reduction of the observed optical energy gap in UV-Vis spectroscopy, both of which indicate the introduction of defect states and changes in the electronic structure. Moreover, AFM results showed smoother surfaces with increased AgO content, indicating improved film uniformity, which may also contribute to the observed changes in carrier transport properties. These results are consistent with previous literature, confirming that the addition of AgO to ZnO thin films can effectively modify the type of electrical conductivity and enhance charge carrier properties by creating trap states and modifying the ZnO lattice structure [29-30].

4. Discussion

The introduction of AgO into ZnO modified the crystal structure by increasing the lattice strain and stimulating secondary phases, as confirmed by X-ray diffraction (XRD) analysis. These structural changes led to the formation of smaller crystals and a higher defect density. FTIR data indicated that AgO doping chemically interacts with the ZnO surface without destroying the structural framework of ZnO, as the Ag–O vibration ranges support successful integration.

AFM confirmed the improvement in film homogeneity at low doping levels, with increased roughness at high concentrations likely due to agglomeration or structural disorder. Optical data showed a narrowing of the energy gap and an increase in light absorption due to defect states and the micro-pressure introduced by AgO.

The Hall effect results confirmed the transition of conductivity type due to the action of the Ag^+ ion as a prospective dopant[31]. The trend in carrier properties aligns with the observed structural and optical changes, confirming that the addition of AgO is an effective strategy for tuning ZnO thin films for electronic and sensory applications.

5. Conclusion

Thin films of $(ZnO)_{1-x}(AgO)_x$ (x = 0.00, 0.05, 0.15, 0.25, 0.30) were deposited using pulsed laser deposition (PLD) on glass substrates. X-ray diffraction (XRD) analysis confirmed the presence of a hexagonal polycrystalline wurtzite-type structure. New peaks associated with silver appeared at higher doping levels, with broadening and shifting of the peaks indicating an

increase in strain and a reduction in crystal size. FTIR spectra showed Zn–O stretching bands, hydroxyl groups, and new bands associated with Ag–O vibrations, confirming the incorporation of AgO. AFM results showed smoother surfaces at low AgO content (x = 0.05, 0.15), while surface roughness increased at higher ratios (x = 0.25, 0.30). UV-Vis measurements indicated that the increase in AgO reduced the transmittance (from 34.83% to 13.86%) and the band gap energy (from 3.2 eV to 2.2 eV), while the absorption coefficient increased. Hall effect measurements showed a transition from n-type to p-type conductivity with modification. The carrier concentration peaked at x = 0.15, while the highest mobility was in the un-doped films and decreased with the addition of AgO.

Acknowledgment

We would like to express my gratitude to the College of Science and the University of Baghdad for their assistance in completing this work by opening the specialized laboratories and providing scientific facilities by the staff of the Physics Department to support the research project.

Conflict of Interest

The authors declare that they have no conflict of interest.

Funding

None.

References

1. Kasai N, Kakudo M, Ahmeda MH, Ahmida NH, Ahmeida AA. Introduction to nanotechnology: Definition, terms, occurrence and applications in environment. Libyan Int Med Univ J. 2017;2(1):12.https://doi.org/10.21502/limuj.003.02.2017
2. Nasrollahzadeh M, Sajadi SM, Sajjadi M, Issaabadi Z. An introduction to nanotechnology. Interface Sci Technol. 2019;28:1–27.https://doi.org/10.1016/B978-0-12-813586-0.00001-8
3. Aadim KA, Mohammad AZ, Abduljabbar MA. Influence of laser energy on synthesizes of CdO nanoparticles in liquid environment. IOP Conf Ser Mater Sci Eng. 2018;454:012028 .https://doi.org/10.1088/1757-899X/454/1/012028
4. Mohammed DT, Mohammed GH. Investigation of structural, optical and electrical properties of MnO doped with Cu thin films prepared by PLD technique for solar cell applications. East Eur J Phys. 2023;(3):391–399.https://doi.org/10.26565/2312-4334-2023-3-42
5. Mosquera AA, Albella JM, Navarro V, Bhattacharyya D, Endrino JL. Effect of silver on the phase transition and wettability of titanium oxide films. Sci Rep. 2016;6:32171. https://doi.org/10.1038/srep32171
6. Dellasega D, Casari CS, Vario F, Conti C, Bottani CE, Bassi AL. Nanostructured Ag_4O_4 thin films produced by ion beam oxidation of silver. Appl Surf Sci. 2013;266:161–169. https://doi.org/10.1016/j.apsusc.2012.11.121
7. Bao K, Zhao Y, Ding W, Xiao Y, Yang B. First principles study of p-type transition and enhanced optoelectronic properties of g-ZnO based on diverse doping strategies. Nanomaterials. 2024;14:1863. https://doi.org/10.3390/nano14231863
8. Yu J, Han W, Suleiman AA, Han S, Miao N, Ling FCC. Recent advances on pulsed laser deposition of large-scale thin films. Small Methods. 2024;8(7):2301282. https://doi.org/10.1002/smtd.202301282
9. Al-Bayati AA, Ali HF. Synthesis, structural, and optical characterization of ZnO/SnO_2 nanocomposites thin films prepared by spin coating and pulse laser deposition. Iraqi J Phys. 2025;23(1):68–77.
10. Cullity BD, Stock SR. Elements of X-ray Diffraction. 3rd ed. New Jersey: Prentice Hall; 2001.
11. Abbas LK. Effect of thickness on structural, morphological, and optical properties for nanocrystalline thin films of $Cd_{1-x}Sn_xS$ for optoelectronic applications. Baghdad Sci J. 2024;21(8):2730–2740.
12. Chitradevi T, Lenus JA, Victor Jaya N. Structure, morphology and luminescence properties of sol–gel synthesized pure and Ag-doped ZnO nanoparticles. Mater Res Express. 2020;7(1):015011.

13. Farha AH, Al Naim AF, Mansour SA. Cost-effective and efficient cool nanopigments based on oleic-acid-surface-modified ZnO nanostructures. Materials. 2023;16(6):2159. https://doi.org/10.3390/ma16062159
14. Matei A, Stoian M, Crăciun G, Țucureanu V. Chemical synthesis and characterization of fatty acid-capped ZnO nanoparticles. J Compos Sci. 2024;8(10):429. https://doi.org/10.3390/jcs8100429
15. Uribe-López MC, Hidalgo-López MC, López-González R, Frías-Márquez DM, Núñez-Nogueira G, Hernández-Castillo D. Photocatalytic activity of ZnO nanoparticles and the role of the synthesis method on their physical and chemical properties. J Photochem Photobiol A Chem. 2021;404:112866. https://doi.org/10.1016/j.jphotochem.2020.112866
16. Abdullwahed MB, Mohammed AM, Ali FF. Synthesis and characterisation of ZnO–Ag thin films and their use as ammonia sensors. Solid State Technol. 2020;63(2).
17. Kumar A, Dhiman P, Singh M. Effect of Fe-doping on the structural, optical and magnetic properties of ZnO thin films prepared by RF magnetron sputtering. Ceram Int. 2016;42:7918–7923. https://doi.org/10.1016/j.ceramint.2016.01.038
18. Godbole R, Godbole VP, Alegaonkar PS, Bhagwat S. Effect of film thickness on gas sensing properties of sprayed WO_3 thin films. New J Chem. 2017;41:11807. https://doi.org/10.1039/C7NJ02460D
19. Obead AH, Abbas NK. Studying the structural and optical properties of $Zn_{1-x}Mg_xO$ nanoparticles. J Opt. 2024;1–14. https://doi.org/10.1007/s12596-024-00323-5
20. Dutta G, Chinnaiyan SK, Sugumaran A, Narayanasamy D. Sustainable bioactivity enhancement of ZnO–Ag nanoparticles in antimicrobial, antibiofilm, lung cancer, and photocatalytic applications. RSC Adv. 2023;13(38):26663–26682. https://doi.org/10.1039/D3RA03521F
21. Dhawale DS, Dubal DP, Phadatare MR, Patil JS, Lokhande CD. Synthesis and characterizations of CdS nanorods by SILAR method: Effect of film thickness. J Mater Sci. 2011;46:5009–5015. https://doi.org/10.1007/s10853-011-5321-5
22. Şahin B, Kaya T. Facile preparation and characterization of nanostructured ZnO/CuO composite thin film for sweat concentration sensing applications. Mater Sci Semicond Process. 2021;121:105428. https://doi.org/10.1016/j.mssp.2020.105428
23. Abbas HH, Hasan BA. The effect of silver oxide on the structural and optical properties of ZnO:AgO thin films. Iraqi J Sci. 2022; 63(4):1526–1539. https://doi.org/10.24996/ijs.2022.63.4.13
24. Gawande MB, Waghmare SR, Gosavi SW. Effect of silver doping on structural, optical and photocatalytic properties of ZnO nanoparticles. RSC Adv. 2024;14(27):19763–19771.
25. Ahmed S, Khan W, Rahman MM, Khan A, Wahab MA, Alshareef SA. Ag-doped ZnO nanorods decorated on graphene-coated flexible substrate for UV detection. Front Chem. 2021;9:661127.
26. Abozied AM, Mostafa AM, Abouelsayed A, Hassan AF, Ramadan AA, Al-Ashkar EA. Preparation, characterization, and nonlinear optical properties of graphene oxide thin film doped with low chirality metallic SWCNTs. J Mater Res Technol. 2021;12:1461–1472. https://doi.org/10.1016/j.jmrt.2021.03.068
27. Ziashahabi A, Prato M, Dang Z, Poursalehi R, Naseri N. The effect of silver oxidation on the photocatalytic activity of Ag/ZnO hybrid plasmonic/metal-oxide nanostructures under visible light and in the dark. Sci Rep. 2019;9(1):11839. https://doi.org/10.1038/s41598-019-48128-z
28. Shah WH, Alam A, Javed H, Rashid K, Ali A, Ali L. Tuning of the band gap and dielectric loss factor by Mn doping of $Zn_{1-x}Mn_xO$ nanoparticles. Sci Rep. 2023;13(1):8646. https://doi.org/10.1038/s41598-023-35987-4
29. Avelar-Muñoz F, Gómez-Rosales R, Ortiz-Hernández AA, Durán-Muñoz H, Berumen-Torres JA, Vagas-Téllez JA. Long electrical stability on dual acceptor p-type ZnO:Ag, N thin films. Micromachines.2024;15(6):800. https://doi.org/10.3390/mi15060800
30. Bao K, Zhao Y, Ding W, Xiao Y, Yang B. First principles study of p-type transition and enhanced optoelectronic properties of g-ZnO based on diverse doping strategies. Nanomaterials. 2024;14(23):1863. https://doi.org/10.3390/nano14231863
31. Kang HS, Ahn BD, Kim JH, Kim GH, Lim SH, Chang HW, Lee SY. Structural, electrical, and optical properties of p-type ZnO thin films with Ag dopant. Appl Phys Lett. 2006;88(20): 202108. https://doi.org/10.1063/1.2203952